Nonrigid Registration and Template Matching for Coronary Motion Modeling from 4D CTA

Dong Ping Zhang[1], Laurent Risser[1,2], Ola Friman[3], Coert Metz[4], Lisan Neefjes[5], Nico Mollet[5], Wiro Niessen[4], and Daniel Rueckert[1]

[1] Department of Computing, Imperial College London, London, UK
[2] Institute for Mathematical Science, Imperial College London, London, UK
[3] Fraunhofer MEVIS, Universitaetsallee 29, 28359 Bremen, Germany
[4] Dept. of Medical Informatics and Radiology, Erasmus MC, Rotterdam, NL
[5] Dept. of Radiology and Cardiology, Erasmus MC, Rotterdam, NL

Abstract. In this paper, we present a method for coronary artery motion tracking in 4D cardiac CT angiogram data sets. The proposed method allows the construction of patient-specific 4D coronary motion model from pre-operative CTA which can be used for guiding totally endoscopic coronary artery bypass surgery (TECAB). The proposed approach consists of three steps: Firstly, the coronary arteries are extracted in the end-diastolic time frame using a minimal cost path approach. To achieve this, the start and end points of the coronaries are identified interactively and the minimal cost path between the start and end points is computed using A* graph search algorithm. Secondly, the cardiac motion is estimated throughout the cardiac cycle by using a non-rigid image registration technique based on a free-form B-spline transformation model and maximization of normalized mutual information. Finally, coronary arteries are tracked automatically through all other phases of the cardiac cycle. This is estimated by deforming the extracted coronaries at end-diastole to all other time frames according the motion field acquired in second step. The estimated coronary centerlines are then refined by template matching algorithm to improve the accuracy. We compare the proposed approach with two alternative approaches: The first approach is based on the minimal cost path extraction of the coronaries with start and end points manually identified in each time frame while the second approach is based on propagating the extracted coronaries from the end-diastolic time frame to other time frames using image-based non-rigid registration only. Our results show that the proposed approach performs more robustly than the non-rigid registration based method and that the resulting motion model is comparable to the motion model constructed from semi-automatic extractions of the coronaries in all time frames.

Keywords: Nonrigid Deformation, Computer Integrated Surgery, Intramodality Registration, Motion Detection and Tracking.

1 Introduction

As one of the leading causes of death worldwide, coronary artery disease occurs due to the failure of the blood circulation to supply adequate oxygen and nu-

B. Fischer, B. Dawant, and C. Lorenz (Eds.): WBIR 2010, LNCS 6204, pp. 210–221, 2010.

trition to cardiac tissues. It is typically caused by the excessive accumulation of atheromatous plaques and fatty deposits within certain regions of the arteries which restricts the blood flow. To treat this disease, arteries or veins grafted from the patient's body are used to bypass the blockages and restore the supply to the heart muscle. Using image-guided robotic surgical system, totally endoscopic coronary artery bypass (TECAB) surgery techniques have been developed to allow clinicians to perform bypass surgery off-pump with three pin-hole incisions in the chest cavity through which two robotic arms and one stereo endoscopic camera are inserted. However, 20-30% conversion rates from TECAB surgery to the conventional invasive surgical approach [1,2] have been reported due to the vessel misidentification and mis-localization caused by the restricted field of view of the stereo endoscopic images.

The goal of our work is to construct a patient-specific 4D coronary artery motion model from preoperative cardiac Computed Tomography Angiography (CTA) sequences. By temporally and spatially aligning this model with intraoperative endoscopic views of the patient's beating heart, this can be used to assist the surgeon to identify and locate the correct coronaries during the TECAB procedures [3,4].

The recent advances in using CTA for the diagnosis of coronary artery disease diagnosis and surgical planning have attracted a wide range of studies. Extensive reviews on coronary artery segmentation are given in Schaap *et al.* [5] and Lesage *et al.* [6]. Although coronary artery segmentation has been well studied, constructing motion models of coronaries from pre-operative scans to assist the diagnosis and surgery is a topic which has received less attention.

In previous work, Shechter *et al.* [7,8] tracked coronary artery motion in a temporal sequence of biplane X-ray angiography images. In their approach, a 3D coronary model is reconstructed from extracted 2D centrelines in end-diastolic angiography images. The deformation throughout the cardiac cycle is then recovered by a registration-based motion tracking algorithm. The disadvantage is that 3D reconstruction of the coronary is required. An alternative approach for the extraction of the coronaries from cardiac CTA has been proposed by Metz *et al.* [9]: Here the coronaries are manually or semi-automatically identified at one time frame and then tracked throughout the cardiac cycle using non-rigid registration of the multi-phase cardiac CTA images. The restriction of this approach is that highly localized motion of the coronaries can not be fully recovered by the motion tracking of the entire heart.

In this paper, we present a novel approach for coronary motion tracking in cardiac CTA images which significantly improves the robustness of motion tracking and reduces the manual interactions. The proposed approach is based on a non-rigid registration of the CTA images which provides an initial estimation of the coronary motion. This estimation is then refined using template fitting algorithm that matches a tubular-like vessel model to the local image region. This simplifies the 4D motion modelling of coronaries significantly. Only one pair of the start and end points of each vessel in end-diastolic frame are manually identified. Once the start and end points have been identified, each coronary branch

from the end-diastolic phase is extracted as the minimal cost path between both points. The proposed approach is compared to a nonrigid image registration based approach similar to the one presented by Metz *et al.* [9] and to manual tracking of the coronaries obtained from graph search at each time frame.

2 Method

We start from presenting the techniques used for pre-processing the images. The main methods are then organized in three parts. Firstly, using Euclidean distance as the heuristic term, A* graph search is performed at each phase in each dataset to extract the minimal cost path of coronaries, based on user-supplied start and end points for each vessel. The extracted results are used as ground truth for evaluating the coronary motion tracking methods. Secondly, we estimate the coronary motion using the hierarchy non-rigid registration of the CTA sequence. Thirdly, the minimal cost coronary paths at end-diastolic phase are transformed to other time points according to the deformation field. The deformed paths are resampled equidistantly and the points from each resampled path are used as initial guesses for vessel template fitting procedure. This enables the tracking of coronary motion without any further user interaction and also estimates the coronary radius at each fitting location. We then compare the template based approach with the non-rigid registration one.

2.1 Image Preprocessing

Before the coronary arteries are extracted their visibility in the cardiac CTA image sequences is enhanced by performing contrast limited adaptive histogram equalization [10]. This improves the contrast and enhances the coronary arteries. Note that this step is carried out for the entire image sequences so that intensities in all time frames are treated similarly and consistently.

Due to the ECG pulsing windows applied in the acquisition and reduced radiation dose [11], the signal-to-noise ration is varying in the multiple-phase 4D data sets. To improve the image quality, 4D anisotropic filtering [12] is used to reduce this noise and preserve the cardiac chamber boundaries and vessel structures. So after histogram equalization, we perform 4D anisotropic diffusion [12] to smooth the image sequence while preserving edges and other salient features. Again, the anisotropic diffusion filtering is performed for the entire 4D image sequence so that neighbouring time frames influence the diffusion at the current time frame.

For the template matching algorithm, minimum and maximum thresholds are used in order to reduce the effect of the presence of inhomogeneous background (e.g. air and tissue mixed region) or irrelevant neighboring structures (e.g. bone or metal implant). Multiple thresholds are selected automatically by 4D multi-level thresholding extended from Otsu's method [13] for each 4D data set. The intensities of the background voxels are increased so that they match the average myocardial intensity level. For the intensities above the upper threshold

level, they are reduced to average myocardium intensity level too. One pair of thresholds is used for each 4D sequence.

2.2 Segmentation of Coronary Centerlines Using Graph Search

We first perform a coarse segmentation of the coronary arteries in the CTA image using a multiscale Hessian-based vessel enhancement filter [14]. The filter utilizes the 2nd-order derivatives of the image intensity after smoothing (using a Gaussian kernel) at multiple scales to identify bright tubular-like structures with various diameters. The six second-order derivatives of the Hessian matrix at each voxel are computed by convolving the image with second-order Gaussian derivatives at a pre-selected scale.

Assuming a 3D image function $I(\mathbf{x})$, the Hessian matrix at a given voxel $\mathbf{x}$ at scale σ is denoted as $H_\sigma(\mathbf{x})$. A vesselness term $V(\mathbf{x})$ is defined as in Frangi *et al.* [14] and is based on the eigenvalues and eigenvectors of $H_\sigma(\mathbf{x})$. The vesselness response is computed at a range of scales. The maximum response with the corresponding optimal scale is obtained for each voxel of the image. Once the vesselness at each voxel is computed, it can be used to define a minimal cost path between the start and end nodes.

The minimal cost path between the start node S and the end node E is obtained using the A* graph search algorithm [15] in the end-diastolic CTA image. The location of the pair of nodes S and E is specified semi-interactively. A uni-directional graph search algorithm evaluates the smallest cost from node S to current node $\mathbf{x}$ denoted as $g(\mathbf{x})$ and the heuristic cost from current node to node E denoted as $h(\mathbf{x})$ to determine which voxel to be selected as next path node. The algorithm finds the optimal path only if the heuristic underestimates the cost. In our approach, the Euclidean distance from $\mathbf{x}$ to E is used to calculate the heuristic cost term. We assess each candidate node by calculating the cost $f(\mathbf{x})$ as:

$$f(\mathbf{x}) = g(\mathbf{x}') + \frac{1}{V(\mathbf{x}) + \epsilon} + \delta h(\mathbf{x}). \tag{1}$$

where $g(\mathbf{x}')$ is the score of the previous node. To initialize the cost function, $g(\mathbf{x}')$ is set to be zero for the start node S. A small positive constant ϵ is added in order to avoid singularities. The parameter δ is estimated as the ratio of the minimum cost of the vessel to the Euclidean distance of the start and end nodes.

By using the heuristic term, the searching space is greatly reduced and the minimum cost path can be found in real-time. When node E is reached, the minimum cost path is reconstructed by tracing backwards to node S. The algorithm finds a minimal cost path consisting of an ordered set of discrete locations (voxels). After extraction of the path we estimate a B-spline representation of coronary centerlines that smoothly interpolates these voxel locations.

2.3 Non-rigid Image Registration for Estimating Coronary Motion

The motion of coronaries during the cardiac cycle is mainly caused by the expansion and contraction of the cardiac chambers. We use non-rigid image

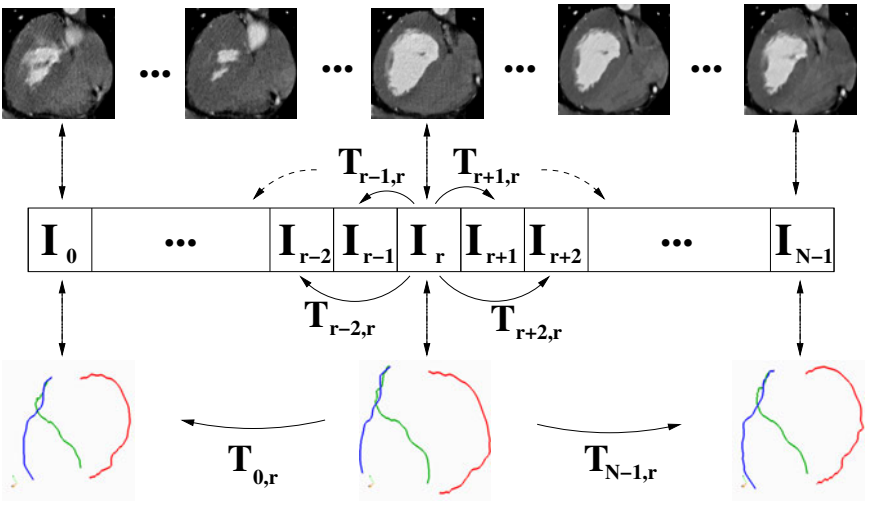

Fig. 1. Illustration of coronary motion tracking using a non-rigid registration approach. The bottom row shows the extracted coronary centerlines from I_r (in the middle) and the transformed centerlines for I_0 and I_{N-1} in the left and right. Right coronary artery is shown in red, left anterior descending artery in green, left circumflex artery in blue.

registration of the cardiac CTA sequence for a first approximation of the coronary motion throughout the cardiac cycle. In our application, we use a non-rigid image registration algorithm which employs a free-form deformation model based on cubic B-splines [16]. A series of registration steps is performed to register each time frame to the reference image at end-diastolic phase. Each registration proceeds in a multi-resolution fashion, starting with a control point spacing of 40mm and ending with a spacing of 5mm. The deformations derived from coarse level are used to initialize the finer level of registration. For each frame we use the registration result from the previous frame as initial estimation as shown in the middle row of Fig. 1. The non-rigid registration algorithm uses normalised mutual information as the similarity measure between time frames. A gradient descent optimization is used to find the optimal transformation. The extracted coronary arteries in the end-diastolic phase are propagated to the other cardiac phases by applying the deformations obtained from the finest registration step as illustrated in the bottom row of Fig. 1.

2.4 Coronary Motion Tracking Using Template Fitting

Combined with the deformation information obtained in Section 2.3, we propose a method for refining the tracking of the coronaries throughout the cardiac CTA sequence based on template localization and fitting. A tubular segment model [17,18] is adopted to map a spatial coordinate $\mathbf{x}$ to the intensity range $[0, 1]$ through a template function $M(\mathbf{x}; r, \mathbf{x}_0, \boldsymbol{v})$. The template function defines an ideal vessel segment centered at point $\mathbf{x}_0$ running in the direction of $\boldsymbol{v}$ with

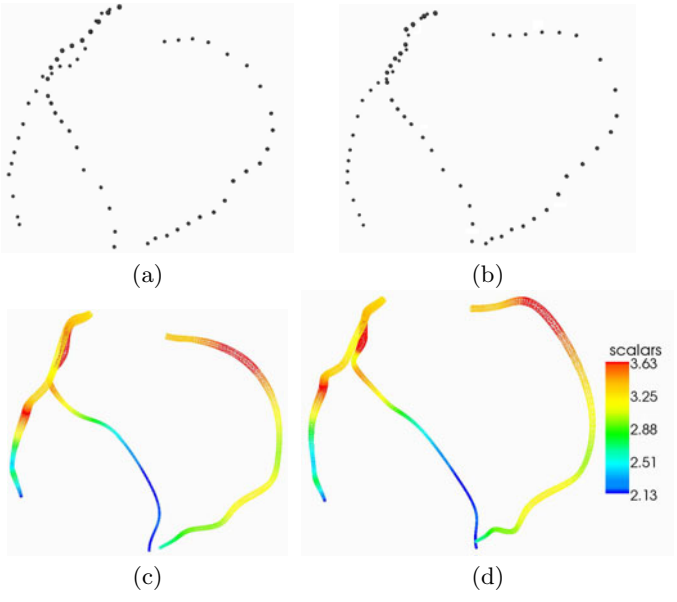

Fig. 2. Combination of non-rigid deformation and template matching. (b) shows the resampled coronary branches extracted at end-disatole as in Section 2.2. (d) shows the vessel lumen by chaining the fitted templates together at end-diastole. (a) shows estimation for the coronary at end-systole. (c) is coronary artery lumen obtained by fitting the templates with corresponding local region in end-systolic CTA image. The varying radii are represented by different colors as in the legend.

radius r. A vessel profile is defined to model the image intensity variation in the cross-sectional plane perpendicular to the vessel direction.

First, an equidistant sample of vessel points from each extracted coronary centerline (Section 2.2) at end-diastolic phase is chosen for refining the coronary segmentation as shown in Fig. 2 (b). Each point from these samples is used as the initial center for the template fitting procedure. For each point, the optimal vessel template together with the corresponding local contrast and local mean intensity parameters are obtained by solving the weighted least squared problem using Levenberg-Marquardt algorithm [18] in the end-diastolic time frame. This provide us a more detailed coronary segmentation with center location, radius, local contrast and mean intensity parameters for each template. By chaining these templates together, we obtain the coronary lumen at end-diastole as shown in Fig. 2 (d).

Given the coronary centrelines extracted in the end-diastolic time frame as shown in the middle bottom of Fig. 1, we can estimate the coronary centerline positions for other time frames by using the deformation information obtained in Section 2.3 to transform the end-diastolic extractions. An equidistant sample of vessel points are chosen from each vessel centerline at each non-end

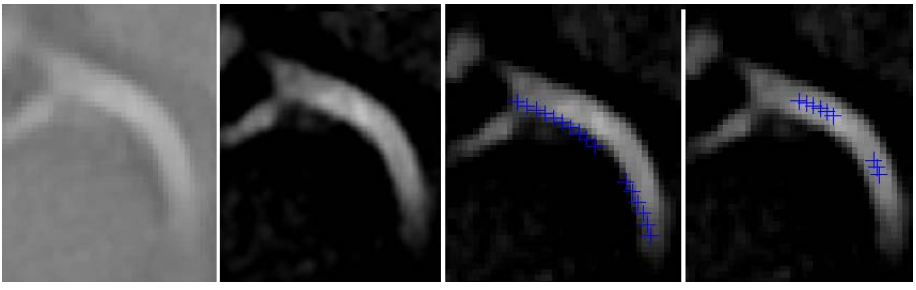

Fig. 3. Illustration of template position estimation and fitting. (a) A small region of CTA image containing right coronary artery. (b) after pre-processing. (c) the estimated right coronary artery position using non-rigid registration. Blue cross shows the estimated vessel centerlines. (d) The vessel centerlines after template fitting. The discontinuity of the centerline is due to that only one slice shown in 2D representation.

diastolic phase as the estimated locations of the centers of the vessel templates. The template fitting algorithm is performed on all these vessel points to provide an accurate match of the template with the local region. To achieve this, the template parameters are optimized again using Levenberg-Marquardt optimization. After this, the new discrete center points and their corresponding radii for each vessel is interpolated using B-spline. The coronary lumen is represented with a tubular mesh. This procedure is repeated in pair-wise order until the coronary lumen in all time frames is obtained. We then quantitatively measure the accuracy of these coronary lumen centerlines by assuming the minimal cost centerlines obtained in Section 2.2 as ground truth. We also compare their difference from the estimated centerlines using only non-rigid registration method as in Section 2.3.

To illustrate the procedure, segmented coronary lumen from two phases are shown in Fig. 2, together with the resampled minimal cost paths which are used as initialization for template matching. For illustration, in Fig. 3, a right coronary artery segment is randomly chosen from one image. It shows template matching improves the accuracy of the estimated centerlines.

3 Results and Evaluation

To assess the performance of the proposed motion tracking strategy we have performed experiments on eight cardiac CTA sequences. Each CTA sequence has twenty phases with various image dimensions ranging from 256×256×89 to 512×512×335 voxels. The voxel dimensions varies from 0.4×0.4×0.5 mm^3 to 0.7×0.7×1.5 mm^3. All datasets have various degrees of artifacts that affect the segmentation and registration procedure. In particular the fast motion of the heart in some time frames can lead to blurring or ghosting artifacts *e.g.* around the coronary artery. As a result of this, in some cases, the non-rigid registration-based approach can only compensate for part of the deformation.

In order to have a gold standard to evaluate the two different motion modeling approaches, the left anterior descending artery (LAD), left circumflex artery (LCX) and right coronary artery (RCA) are extracted using the graph search algorithm (Section 2.2) from eight CTA sequences, P1, P2, P3, P4, P5, P6, P7 and P8. In all eight patients, the start and end points of the vessels have been identified manually and the results of the minimal cost path extraction have been judged as correctly falling inside the vessel lumen. The accuracy of these extractions are restricted by the shortcut effect as shown in [19]. The results are compared with motion estimates of the LAD, LCX and RCA as obtained using the non-rigid registration and template matching based approaches.

In order to assess the quality of motion tracking results, the distance between the semi-automatic extracted minimal cost centerline M and tracked coronary centerline U of each coronary branch in each time frame is measured. The distance is defined as,

$$D\,(M,\,U)\;=\;\frac{1}{N_M}\sum_{i=1}^{N_M}\|m_i - l(m_i,U)\|_2 + \frac{1}{N_U}\sum_{j=1}^{N_U}\|u_j - l(u_j,M))\|_2 \quad (2)$$

where N_M and N_U are the number of points representing vessel M and vessel U correspondingly. For each point $m_i \in M$, $l(m_i,\,U)$ calculates the closest point of m_i on the automatically extracted vessel U. Similarly, for each point $u_j \in U$, $l(u_j,\,M)$ defines the closest point of u_j on the vessel M.

The results are shown in Fig. 4. The total displacement of each coronary artery is computed as the distance between the minimal-cost centerline at end-diastole phase and the minimal-cost centerline at each other phase and is shown in the first column (a). The second column (b) shows the tracking error from purely non-rigid registration based approach. It is measured as the distance between centrelines estimated via non-rigid registration and the gold standard for each phase. The third column (c) shows the tracking error using the registration and template matching combined approach. It is measured as the distance between centrelines estimated via the proposed method and the gold standard for each phase.

We compare the accuracy of non-rigid registration based tracking method with the proposed approach in Table 1. The average motion is calculated as the average of the total displacements of each coronary artery for each patient. Mean error 1 shows the average residual motion for the non-rigid registration based tracking method. Mean error 2 shows the average residual motion for the non-rigid registration and template-matching based approach.

We also consider that the motion tracking is successful when the distance between modeled coronary and the minimal-cost path is under 1.4mm which is twice of the voxel size for most testing data sets. By considering this error threshold for right coronary artery motion modeling, 92% of vessel tracking are performed successfully by using our proposed method, comparing with 46% when using the purely non-rigid registration approach. By choosing 2.8 mm as threshold, all the right coronary tracking are successful in our method while the non-rigid registration approach produces 72% success rate. From Fig. 4 and Table 1, we can conclude that combining the non-rigid registration with the

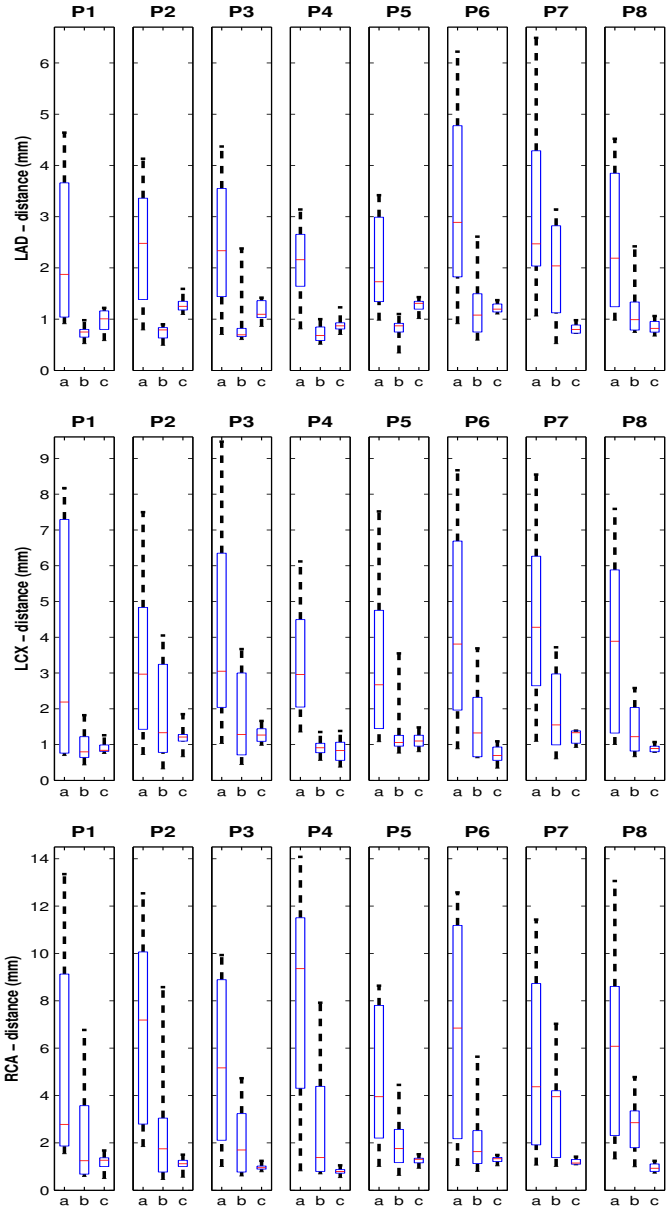

Fig. 4. Comparison of coronary motion tracking results. The total coronary displacement (LAD, LCX, RCA) is shown in column (a). The residual coronary displacement after non-rigid registration is shown in column (b) and after the combined registration and template-based tracking is shown in column (c). The results show that the proposed tracking method is able to model the coronary motion with acceptable errors (under 2 voxels) and in most cases it performed better.

Table 1. Average coronary motion and mean errors of motion tracking

LAD

	P1	P2	P3	P4	P5	P6	P7	P8
Average Motion (mm)	2.39	2.40	2.53	2.12	2.06	3.26	3.29	2.43
Mean error 1 (mm)	0.74	0.73	0.90	0.72	0.79	1.23	2.01	1.15
Mean error 2 (mm)	0.97	1.27	1.14	0.90	1.27	1.21	0.81	0.84

LCX

	P1	P2	P3	P4	P5	P6	P7	P8
Average Motion (mm)	3.41	3.23	4.42	3.28	3.10	4.31	4.47	3.92
Mean error 1 (mm)	0.92	1.81	1.77	0.90	1.31	1.61	1.89	1.45
Mean error 2 (mm)	0.90	1.19	1.28	0.84	1.12	0.72	1.21	0.89

RCA

	P1	P2	P3	P4	P5	P6	P7	P8
Average Motion (mm)	5.53	6.83	5.33	8.14	4.89	6.62	5.44	5.96
Mean error 1 (mm)	2.35	2.62	2.19	2.83	1.90	2.27	3.23	2.68
Mean error 2 (mm)	1.19	1.10	0.95	0.79	1.26	1.29	1.19	0.94

template matching together improve the motion tracking accuracy in most cases, particularly in the frames when the rapid cardiac motion occurs. The variance of tracking error is greatly reduced by using the proposed method.

4 Conclusions and Future Work

We have presented a novel approach for patient-specific coronary artery motion modeling from cardiac CTA sequences which combines the template matching and non-rigid registration algorithm. The proposed method has been tested on eight clinical CTA datasets and proved to be more robust than purely non-rigid registration approach. The limitation of this study is the lack of manual annotated coronary centerlines and lumen for the CTA images. By assuming the semi-automatically extracted minimal-cost paths as ground truth, the accuracy of the proposed tracking method is potentially under-estimated particularly for LAD and LCX. For more accurate evaluation, manual annotations are needed. However, it is very time-consuming and laborious to have all coronaries manually annotated in large CTA image. More importantly, in our application we focus more on the motion tracking of the coronaries from 4D pre-operative CTA scans. The vesselness based graph search algorithm provides us reliable and fast coronary artery extractions to be used as ground truth.

By constructing a 4D motion model of the coronaries from pre-operative cardiac images and aligning the 4D coronary model with the series of 2D endoscopic images acquired during the operation, we aim to assist the surgical planning and

provide image guidance in robotic-assisted totally endoscopic coronary artery bypass (TECAB) surgery. Through this work, we expect to reduce the conversion rate from TECAB to conventional invasive procedures.

References

1. Mohr, F.W., Falk, V., Diegeler, A., Walther, T., Gummert, J.F., Bucerius, J., Jacobs, S., Autschbach, R.: Computer-enhanced "robotic" cardiac surgery: Experience in 148 patients. Journal of Thoracic and Cardiovascular Surgery 121(5), 842–853 (2001)
2. Dogan, S., Aybek, T., Andressen, E., Byhahn, C., Mierdl, S., Westphal, K., Matheis, G., Moritz, A., Wimmer-Greinecker, G.: Totally endoscopic coronary artery bypass grafting on cardiopulmonary bypass with robotically enhanced telemanipulation: Report of forty-five cases. Journals of Thoracic Cardiovascular Surgery 123, 1125–1131 (2002)
3. Figl, M., Rueckert, D., Hawkes, D., Casula, R., Hu, M., Pedro, O., Zhang, D.P., Penney, G., Bello, F., Edwards, P.: Augmented reality image guidance for minimally invasive coronary artery bypass. In: Proc. SPIE, vol. 6918 (2008)
4. Figl, M., Rueckert, D., Hawkes, D., Casula, R., Hu, M., Pedro, O., Zhang, D., Penney, G., Bello, F., Edwards, P.: Image guidance for robotic minimally invasive coronary artery bypass. Computerized Medical Imaging and Graphics 34, 61–68 (2009)
5. Schaap, M., Metz, C.T., van Walsum, T., van der Giessen, A.G., Weustink, A.C., Mollet, N.R., Bauer, C., Bogunovifa, H., Castro, C., Deng, X., Dikici, E., ODonnell, T., Frenay, M., Friman, O., Hernandez Hoyos, M., Kitslaar, P.H., Krissian, K., Kuhnel, C., Luengo-Oroz, M.A., Orkisz, M., Smedby, O., Styner, M., Szymczak, A., Tek, H., Wang, C., Warfield, S.K., Zambal, S., Zhang, Y., Krestin, G.P., Niessen, W.J.: Standardized evaluation methodology and reference database for evaluating coronary artery centerline extraction algorithms. Medical Image Analysis 13(5), 701–714 (2009)
6. Lesage, D., Angelini, E.D., Funka-Lea, G., Bloch, I.: A review of 3D vessel lumen segmentation techniques: Models, features and extraction schemes. Medical Image Analysis 13, 819–845 (2009)
7. Shechter, G., Devernay, F., Quyyumi, A., Coste-Maniere, E., McVeigh, E.: Three-dimensional motion tracking of coronary arteries in biplane cineangiograms. IEEE Transactions in Medical Imaging 22(4), 493–603 (2003)
8. Shechter, G., Resar, J.R., McVeigh, E.R.: Displacement and velocity of the coronary arteries: cardiac and respiratory motion. IEEE Transactions on Medical Imaging 25, 369–375 (2006)
9. Metz, C., Schaap, M., Klein, S., Neefjes, L., Capuano, E., Schultz, C., van Geuns, R.J., Serruys, P.W., van Walsum, T., Niessen, W.J.: Patient specific 4D coronary models from ECG-gated CTA data for intra-operative dynamic alignment of CTA with X-ray images. In: Yang, G.-Z., Hawkes, D., Rueckert, D., Noble, A., Taylor, C. (eds.) MICCAI 2009. LNCS, vol. 5761, pp. 369–376. Springer, Heidelberg (2009)
10. Zuiderveld, K.: Contrast limited adaptive histogram equalization. In: Graphics gems IV, pp. 474–485. Academic Press Professional, Inc., San Diego (1994)

11. Weustink, A.C., Mollet, N.R., Pugliese, F., Meijboom, W.B., Nieman, K., Heijenbrok-Kal, M.H., Flohr, T.G., Neefjes, L.A., Cademartiri, F., de Feyter, P.J., Krestin, G.P.: Optimal electrocardiographic pulsing windows and heart rate: Effect on image quality and radiation exposure at dual-source coronary CT angiography. Radiology 248(3), 792–798 (2008)
12. Weickert, J.: Anisotropic Diffusion In Image Processing. Teubner-Verlag, Stuttgart (1998)
13. Otsu, N.: A threshold selection method from gray-level histograms. IEEE Transactions on Systems, Man and Cybernetics 9(1), 62–66 (1979)
14. Frangi, A., Niessen, W., Hoogeveen, R., van Walsum, T., Viergever, M.: Model-based quantitation of 3D magnetic resonance angiographic images. IEEE Transactions on Medical Imaging 18(10), 946–956 (1999)
15. Hart, P.E., Nilsson, N.J., Raphael, B.: A formal basis for the heuristic determination of minimum cost paths. IEEE Transactions on Systems Science and Cybernetics 4(2), 100–107 (1968)
16. Rueckert, D., Sonoda, L.I., Hayes, C., Hill, D.L., Leach, M.O., Hawkes, D.J.: Non-rigid registration using free-form deformations: application to breast MR images. IEEE Transactions on Medical Imaging 18(8), 712–721 (1999)
17. Friman, O., Hindennach, M., Peitgen, H.O.: Template-based multiple hypotheses tracking of small vessels. In: 5th IEEE International Symposium on Biomedical Imaging: From Nano to Macro, pp. 1047–1050 (2008)
18. Friman, O., Hindennach, M., Khnel, C., Peitgen, H.O.: Multiple hypothesis template tracking of small 3d vessel structures. Medical Image Analysis (December 2009)
19. Li, H., Yezzi, A.: Vessels as 4d curves: Global minimal 4d paths to extract 3d tubular surfaces. In: Conference on Computer Vision and Pattern Recognition Workshop, CVPRW 2006, p. 82 (June 2006)